

# 1/(N - 1) Expansion Approach to Full-counting Statistics for the SU(N) Anderson Model

Akira Oguri

*Department of Physics, Osaka City University, Sumiyoshi-ku, Osaka, Japan*

Rui Sakano

*Institute for Solid State Physics, University of Tokyo, Kashiwa, Chiba, Japan*

(Dated: February 13, 2018)

We apply a recently developed  $1/(N - 1)$  expansion to the full-counting statistics for the  $N$ -fold degenerate Anderson impurity model in the Kondo regime. This approach is based on the perturbation theory in the Coulomb interaction  $U$  and is different from the conventional large- $N$  theories, such as the usual  $1/N$  expansion and non-crossing approximation. We have confirmed that the calculations carried out up to order  $1/(N - 1)^2$  agree closely with those of the numerical renormalization group at  $N = 4$ , where the degeneracy is still not so large. This ensures the applicability of our approach for  $N \geq 4$ . We present the results of the cumulants of the probability distribution function for a nonequilibrium current through a quantum dot in the particle-hole symmetric case.

PACS numbers: 72.15.Qm, 73.63.Kv, 75.20.Hr

Keywords: Kondo effect, Quantum dot, Orbital degeneracy, Nonequilibrium current

## I. INTRODUCTION

The universal Kondo behavior in quantum dots has been studied intensively for a nonequilibrium current [1–6] and shot noise [7–13]. The effects of orbital degeneracy on the universality have also been a subject of current interest [14–18].

The essential features of the low-energy properties of orbital systems may be deduced from the SU( $N$ ) Anderson model, for which  $N = 2$  corresponds to the spin degeneracy. The exact numerical renormalization group (NRG) approach [19] has been applied to this model for small degeneracies  $N \leq 4$  [20]. For  $N > 4$ , the conventional large- $N$  theories, such as the  $1/N$  expansion and the non-crossing approximation [21, 22], are applicable to a wide energy scale except for the low-energy Fermi-liquid regime. Therefore, at low energies, alternative approaches are needed to explore the universal behavior for  $N > 4$ .

Recently, we proposed a different type of large- $N$  theory, by using a scaling that takes  $u = (N - 1)U$  as an independent variable instead of the bare Coulomb interaction  $U$  [23, 24]. The factor  $N - 1$  represents the number of interacting orbitals, excluding the one prohibited by the Pauli principle. With this scaling, the perturbation series in  $U$  can be reorganized as an expansion in powers of  $1/(N - 1)$ . To leading order in  $1/(N - 1)$ , it describes the Hartree-Fock random phase approximation (HF-RPA). The higher-order corrections systematically describe the fluctuations beyond the HF-RPA. As the unperturbed Hamiltonian includes the tunneling matrix element between the impurity and the conduction bands, this approach naturally describes the Fermi-liquid state.

In this report, we discuss dependences of the renormalized parameters on the degeneracy  $N$ , carrying out the calculations up to order  $1/(N - 1)^2$ . Furthermore, we apply this approach to the full-counting statistics [25–

27] for the nonequilibrium current distribution through quantum dots in the Kondo regime.

## II. MODEL AND FORMULATION

We consider the SU( $N$ ) impurity Anderson model with a finite interaction  $U$  connected to two leads ( $\nu = L, R$ ):  $\mathcal{H} = \mathcal{H}_0 + \mathcal{H}_U$ ,

$$\mathcal{H}_0 = \sum_{m=1}^N \xi_d d_m^\dagger d_m + \sum_{\nu=L,R} \sum_{m=1}^N \int_{-D}^D d\epsilon \epsilon c_{\epsilon\nu m}^\dagger c_{\epsilon\nu m} + \sum_{\nu=L,R} \sum_{m=1}^N v_\nu \left( d_m^\dagger \psi_{\nu m} + \psi_{\nu m}^\dagger d_m \right), \quad (1)$$

$$\mathcal{H}_U = \sum_{m \neq m'} \frac{U}{2} \left( n_{dm} - \frac{1}{2} \right) \left( n_{dm'} - \frac{1}{2} \right). \quad (2)$$

Here,  $\xi_d = \epsilon_d + (N - 1)U/2$ ,  $d_m^\dagger$  is the creation operator for an electron with energy  $\epsilon_d$  and orbital  $m$  ( $= 1, 2, \dots, N$ ) in the impurity site, and  $n_{dm} = d_m^\dagger d_m$ . The operator  $c_{\epsilon\nu m}^\dagger$  for a conduction electron in the lead  $\nu$  is normalized as  $\{c_{\epsilon\nu m}, c_{\epsilon'\nu' m'}^\dagger\} = \delta_{\nu\nu'} \delta_{mm'} \delta(\epsilon - \epsilon')$ , and  $\psi_{\nu m} = \int_{-D}^D d\epsilon \sqrt{\rho} c_{\epsilon\nu m}$ . The hybridization energy scale is given by  $\Delta \equiv \Gamma_L + \Gamma_R$ , with  $\Gamma_\nu = \pi \rho v_\nu^2$  and  $\rho = 1/(2D)$ .

We use the imaginary-frequency Green's function that is given, for  $|\omega| \ll D$ , by

$$G(i\omega) = \frac{1}{i\omega - \xi_d + i\Delta \operatorname{sgn} \omega - \Sigma(i\omega)}. \quad (3)$$

Here,  $\Sigma(i\omega)$  is the self-energy due to  $\mathcal{H}_U$ . The ground-state average of the local charge,  $\langle n_{dm} \rangle = \delta/\pi$ , can be deduced from the phase shift  $\delta \equiv \cot^{-1}(E_d^*/\Delta)$  with  $E_d^* \equiv \xi_d + \Sigma(0)$ . The renormalized parameters are defined by  $1/z \equiv 1 - \partial \Sigma(i\omega)/\partial(i\omega)|_{\omega=0}$ ,  $\tilde{\epsilon}_d \equiv z E_d^*$ , and

$$\text{wavy line} = \text{wavy line} + \text{bubble} + \text{two bubbles} + \dots$$

FIG. 1: The leading order diagrams in the  $1/(N-1)$  expansion. The wavy and the solid lines indicate  $U$  and  $G_0$ , respectively. The double wavy line represents  $\mathcal{U}_{\text{bub}}(i\omega)$ .



FIG. 2: The order  $1/(N-1)$  vertex and self-energy.

$\tilde{\Delta} \equiv z\Delta$ . Furthermore, the enhancement factors for the spin and charge susceptibilities,  $\tilde{\chi}_s \equiv \tilde{\chi}_{mm} - \tilde{\chi}_{mm'}$  and  $\tilde{\chi}_c \equiv \tilde{\chi}_{mm} + (N-1)\tilde{\chi}_{mm'}$ , can be expressed in terms of  $z$  and the vertex function  $\Gamma_{mm';m'm}(i\omega_1, i\omega_2; i\omega_3, i\omega_4)$  for  $m \neq m'$  [28, 29]:

$$\tilde{\chi}_{mm} = \frac{1}{z}, \quad \tilde{\chi}_{mm'} = -\frac{\sin^2\delta}{\pi\Delta} \Gamma_{mm';m'm}(0, 0; 0, 0), \quad (4)$$

and  $\tilde{U} \equiv z^2\Gamma_{mm';m'm}(0, 0; 0, 0)$  for  $m \neq m'$  represents the residual interaction between the quasi-particles.

We introduce a scaling for the bare and the renormalized interactions with a factor  $N-1$  of [23, 24]:

$$g \equiv \frac{(N-1)U}{\pi\Delta}, \quad \tilde{g} \equiv \frac{(N-1)\tilde{U}}{\pi\tilde{\Delta}}. \quad (5)$$

With these parameters, the Wilson ratio  $R \equiv z\tilde{\chi}_s$  and that for the charge sector can be expressed in the form,

$$R = 1 + \frac{\tilde{g}}{N-1} \sin^2\delta, \quad z\tilde{\chi}_c = 1 - \tilde{g} \sin^2\delta. \quad (6)$$

One of the merits of this scaling is that the perturbation expansion with respect to  $\mathcal{H}_U$  can be classified according to the power of  $1/(N-1)$ , taking  $g$  as an independent variable. In the present report, we consider the particle-hole symmetric case:  $\epsilon_d = -(N-1)U/2$  and  $\delta = \pi/2$ .

### III. EXPANSION UP TO ORDER $1/(N-1)^2$

At zero order with respect to  $1/(N-1)$ , the limit of  $N \rightarrow \infty$  is taken at fixed  $g$ , and it gives the Hartree-Fock results. Specifically, at half-filling, the unperturbed Green's function is given by  $G_0(i\omega) = [i\omega + i\Delta \text{sgn } \omega]^{-1}$  as  $\xi_d = 0$ .

The leading-order corrections in the  $1/(N-1)$  expansion arise from a series of bubble diagrams,  $\mathcal{U}_{\text{bub}}(i\omega)$ , of the RPA types shown in Fig. 1:

$$\mathcal{U}_{\text{bub}}(i\omega) = U + U \sum_{k=1}^{\infty} \mathcal{A}_k \left[ -U \chi_0(i\omega) \right]^k. \quad (7)$$

Here,  $\chi_0(i\omega) = -\int \frac{d\omega'}{2\pi} G_0(i\omega + i\omega') G_0(i\omega')$ , and the coefficient  $\mathcal{A}_k = (N-1)^k \sum_{p=0}^k [-1/(N-1)]^p$  arises from

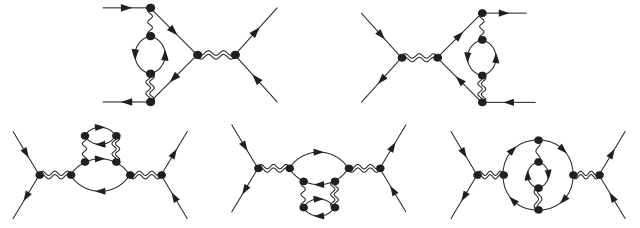


FIG. 3: The order  $1/(N-1)^2$  diagrams for the vertex function  $\Gamma_{mm';m'm}(0, 0; 0, 0)$  for  $m \neq m'$  at half-filling  $\xi_d = 0$ .

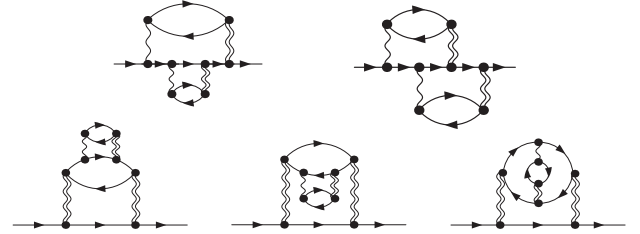


FIG. 4: The order  $1/(N-1)^2$  self-energy at half-filling.

the summation over the orbital indices for a series of  $k$  fermion loops. Correspondingly, the order  $1/(N-1)$  contributions of  $\Gamma_{mm';m'm}(0, 0; 0, 0)$  arise from the first diagram in Fig. 2, and give the leading-order correction to the renormalized coupling as

$$\tilde{g} = \frac{g}{1+g} + O\left(\frac{1}{N-1}\right). \quad (8)$$

This correction determines the Wilson ratio  $R$  to order  $1/(N-1)$  through Eq. (6). Similarly, the order  $1/(N-1)$  self-energy arises from the second diagram in Fig. 2.

Higher-order fluctuations beyond the RPA appear first through the next-leading-order contributions. Figures 3 and 4 show the order  $1/(N-1)^2$  diagrams for the vertex function and the self-energy in the particle-hole symmetric case, respectively. These contributions and the higher-order components from Eq. (7) determine the renormalization factor  $z$  and the Wilson ratio  $R$  to order  $1/(N-1)^2$ . In the present work, we have calculated all these next-leading-order contributions. An outline of the calculations is given in a previous paper [24]. We have also carried out the NRG calculations for  $N=4$  to demonstrate the reliability of the  $1/(N-1)$  expansion.

Figure 5 shows the next-leading-order results for  $\tilde{g}$  and  $z$ , plotted as functions of  $g$ . We see the very close agreement between the NRG and the next-leading-order results in the  $1/(N-1)$  expansion for  $N=4$ , especially for the renormalized coupling  $\tilde{g}$ . The two curves for  $\tilde{g}$ , for  $N=4$ , almost overlap each other over the whole range of  $g$  although the next-leading-order results (green dashed line) are slightly smaller than those of the NRG (solid circles). As  $N$  increases,  $\tilde{g}$  converges rapidly to the RPA value,  $\tilde{g} \rightarrow g/(1+g)$ , which is asymptotically exact in the limit of  $N \rightarrow \infty$ . We also see that the value that  $\tilde{g}$  can take is bounded in a very narrow region between the curve for  $N=4$  and that for the  $N \rightarrow \infty$  limit.

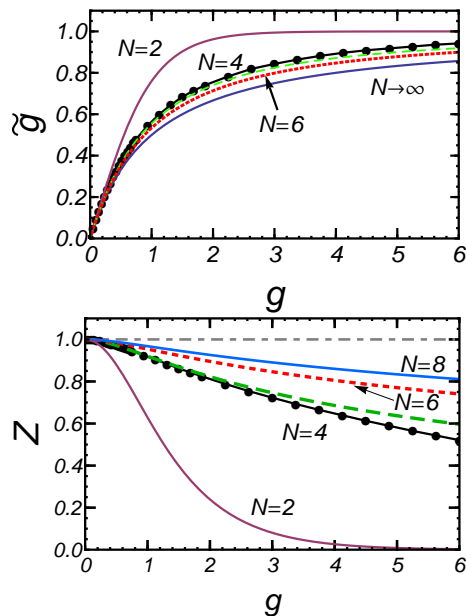


FIG. 5: (Color online) Renormalized parameters  $\tilde{g}$  and  $z$  in the particle-hole symmetric case  $\epsilon_d = -(N-1)U/2$  are plotted as functions of the scaled Coulomb interaction  $g$  for  $N=2$  (Bethe ansatz [30]), and for  $N=4, 6, 8$  (next-leading order in the  $1/(N-1)$  expansion). For  $N=4$ , the NRG results [16, 31] are also shown with the solid circles ( $\bullet$ ). In the  $N \rightarrow \infty$  limit,  $\tilde{g}$  and  $z$  approach  $\tilde{g} \rightarrow g/(1+g)$  and  $z \rightarrow 1.0$ .

The order  $1/(N-1)^2$  results for the renormalization factor  $z$ , shown in Fig. 5, also agree well with the NRG results for  $N=4$  at  $g \lesssim 3.0$ , or equivalently in the region where  $\tilde{g} \lesssim 0.8$ . This indicates that the next-leading-order results also reproduce the Kondo energy scale,  $\tilde{\Delta} = z\Delta$ , properly from the weak-coupling to intermediate-coupling regions where  $\tilde{g}$  is still not very close to 1.0, the value in the strong coupling limit.

#### IV. FULL-COUNTING STATISTICS

The  $1/(N-1)$  expansion can be applied to nonequilibrium transport at finite bias voltages  $V$ . To be specific, we choose the lead-dot couplings and chemical potentials in the leads to be symmetric,  $\Gamma_L = \Gamma_R$  and  $\mu_L = -\mu_R$  ( $= eV/2$ ), and consider a steady state in the particle-hole symmetric case. In this case, the retarded Green's function, which is asymptotically exact at low energies up to terms of order  $\omega^2$ ,  $T^2$ , and  $(eV)^2$ , is given by [4, 16]

$$G^r(\omega) \simeq \frac{z}{\omega + i\tilde{\Delta} + i\frac{\tilde{g}^2}{2(N-1)\tilde{\Delta}} [\omega^2 + \frac{3}{4}(eV)^2 + (\pi T)^2]}. \quad (9)$$

The average and the fluctuations of the steady current at low energies can be described by the local Fermi-liquid theory, which follows from this form of the Green's func-

tion. The Fermi-liquid theory, or the related renormalized perturbation theory (RPT) [32], can also be applied to the full-counting statistics for nonequilibrium transport. Specifically, we consider the probability distribution  $P(\mathbf{q})$  of the transferred charge  $\mathbf{q} = (q_1, q_2, \dots, q_N)$  from the left lead to the orbital  $m$  of the Anderson impurity during a time interval  $\mathcal{T}$ . The generating function for this probability distribution is defined by  $\chi(\boldsymbol{\lambda}) = \sum_{\mathbf{q}} e^{i\boldsymbol{\lambda} \cdot \mathbf{q}} P(\mathbf{q})$  with the counting fields  $\boldsymbol{\lambda} = (\lambda_1, \lambda_2, \dots, \lambda_N)$ , and can be expressed in the form [25]

$$\chi(\boldsymbol{\lambda}) = \left\langle T_C \exp \left\{ -i \int_C dt [\mathcal{H}_T^\lambda(t) + \mathcal{H}_U(t)] \right\} \right\rangle. \quad (10)$$

Here,  $T_C$  is the time-ordering operator along the Keldysh contour  $C$ , and the time evolution is defined with respect to an extended Hamiltonian  $\mathcal{H}^\lambda(t) = \mathcal{H}_0 + \mathcal{H}_T^\lambda(t) + \mathcal{H}_U$ :

$$\mathcal{H}_T^\lambda(t) = \sum_{km} \left[ v_L e^{i\lambda_m(t)/2} d_m^\dagger c_{kLm} + v_R d_m^\dagger c_{kRm} \right] + \text{H.c.} \quad (11)$$

Here, the counting field depends on the path such that  $\lambda_m(t_\mp) = \pm\lambda_m$  for the forward ( $t_-$ ) and backward ( $t_+$ ) paths, respectively, and is switched on during a time interval  $[t: 0 \rightarrow \mathcal{T} \rightarrow 0]$ .

We obtained an explicit expression of  $\chi(\boldsymbol{\lambda})$ , which is asymptotically exact at low energies up to order  $(eV)^3$  for general  $N$  and  $U$ , using the RPT [17, 18]. The cumulant for the full current can be derived from  $\chi(\boldsymbol{\lambda})$ , choosing the counting fields to be  $\lambda_m = \lambda$  for all  $m$  and then taking a derivative  $\mathcal{C}_n = (-i)^n \frac{d^n}{d\lambda^n} \ln \chi(\lambda)$ :

$$\frac{\mathcal{C}_n}{\mathcal{T}} = \frac{J_u}{e} \left[ \delta_{1n} + \frac{(-1)^n}{12} \left\{ 1 + \frac{(1+2^{n+1})\tilde{g}^2}{(N-1)} \right\} \left( \frac{eV}{\tilde{\Delta}} \right)^2 \right]. \quad (12)$$

Here,  $J_u = Ne^2V/(2\pi\hbar)$  is the linear-response current of the unitary limit, and  $\delta_{nn'}$  is the Kronecker's delta. Equation (12) shows that the nonequilibrium properties can also be characterized by the two renormalized parameters,  $\tilde{g}$  and the Kondo energy scale  $\tilde{\Delta}$ , at low energies in the particle-hole symmetric case. For  $n=1$ , the cumulant  $e\mathcal{C}_1/\mathcal{T}$  expresses the steady current. The universal properties of the cumulants for  $n \geq 2$  can be extracted from the Fano-factor-inspired ratio (FFIR), which is normalized with respect to the backscattering current  $J_b \equiv J_u - e\mathcal{C}_1/\mathcal{T}$  [10]:

$$\frac{\mathcal{C}_n}{\mathcal{C}_n^P} = \frac{1 + \frac{(1+2^{n+1})\tilde{g}^2}{N-1}}{1 + \frac{5\tilde{g}^2}{N-1}}, \quad \frac{\mathcal{C}_n^P}{\mathcal{T}} \equiv (-1)^n \frac{J_b}{e}. \quad (13)$$

Here,  $\mathcal{C}_n^P$  can also be regarded as the Poisson value of the cumulant, and the FFIR for  $n=2$  corresponds to the Fano factor [16].

Figure 6 shows the ratios  $\mathcal{C}_n/\mathcal{C}_n^P$  for the noise  $n=2$  (top), the skewness  $n=3$  (middle), and sharpness  $n=4$

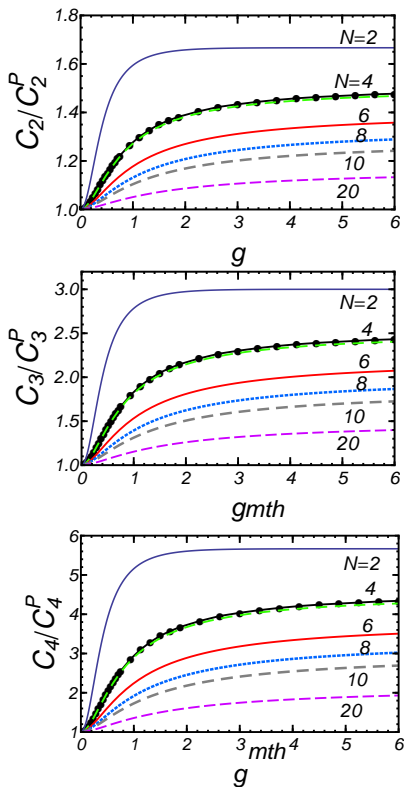


FIG. 6: (Color online) The FFIR  $C_n/C_n^P$  for  $n = 2$  (top),  $n = 3$  (middle), and  $n=4$  (bottom) are plotted as functions of  $g$  for  $N = 2$  (Bethe ansatz), and  $N = 4, 6, 8, 10, 20$  (next-leading-order results in the  $1/(N - 1)$  expansion). The NRG results (solid circles) are also shown for  $N = 4$ .

(bottom) as functions of the scaled Coulomb interaction  $g$  for several value of the orbital degeneracy  $N$ . We see close agreement between the NRG and the next-leading-order results for  $N = 4$  again. As the next-leading-order  $1/(N - 1)$  results for  $\tilde{g}$  are numerically almost exact for  $N \geq 4$ , the results shown in Fig. 6 capture orbital effects correctly. In the strong coupling limit  $g \rightarrow \infty$ , the FFIR approaches  $C_n/C_n^P \rightarrow (N + 2^{n+1})/(N + 4)$  as the renormalized coupling converges to  $\tilde{g} \rightarrow 1$ . As  $N$  increases,  $\tilde{g}$  converges rapidly to the value of  $\tilde{g} \simeq g/(1 + g)$  as mentioned above. Thus, for  $N \gtrsim 8$ , the  $N$  dependence is determined essentially by the factor  $1/(N - 1)$  appearing explicitly in Eq. (13). In the limit of  $N \rightarrow \infty$ , the cumulant approaches the Poisson value  $C_n/C_n^P \rightarrow 1$  as the fluctuations due to electron correlations are suppressed and the mean-field theory becomes asymptotically exact.

In summary, carrying out the  $1/(N - 1)$  expansion up to order  $1/(N - 1)^2$ , we have obtained the cumulants for the probability distribution of the current through a quantum dot with orbital degeneracy  $N > 4$  at low energies. The results of the renormalized coupling  $\tilde{g}$  show excellent agreement at  $N = 4$  with the exact NRG results in the particle-hole symmetric case. This enable us to obtain *almost* exact numerical results for the Fano-factor-inspired ratio  $C_n/C_n^P$  for  $N > 4$ .

#### Acknowledgments

The authors thank T. Fujii, T. Kato, and A. C. Hewson for discussions. This work is supported by JSPS Grants-in-Aid for Scientific Research C (No. 23540375, and No. 24540316). Numerical computation was partly carried out at the Yukawa Institute Computer Facility.

- 
- [1] M. Grobis, I. G. Rau, R. M. Potok, H. Shtrikman, and D. Goldhaber-Gordon, Phys. Rev. Lett. **100**, 246601 (2008).
  - [2] G. D. Scott, Z. K. Keane, J. W. Ciszek, J. M. Tour, and D. Natelson, Phys. Rev. B **79**, 165413 (2009).
  - [3] A. Kaminski, Yu. V. Nazarov, and L. I. Glazman, Phys. Rev. B **62**, 8154 (2000).
  - [4] A. Oguri, Phys. Rev. B **64**, 153305 (2001).
  - [5] T. Fujii and K. Ueda, Phys. Rev. B **68**, 155310 (2003).
  - [6] A. C. Hewson, J. Bauer, and A. Oguri, J. Phys.: Condens. Matter **17**, 5413 (2005).
  - [7] O. Zarchin, M. Zaffalon, M. Heiblum, D. Mahalu, and V. Umansky, Phys. Rev. B **77**, 241303 (2008).
  - [8] Y. Yamauchi, K. Sekiguchi, K. Chida, T. Arakawa, S. Nakamura, K. Kobayashi, T. Ono, Teruo, T. Fujii, and R. Sakano, Phys. Rev. Lett. **106**, 17660 (2011).
  - [9] A. O. Gogolin and A. Komnik, Phys. Rev. B **73**, 195301 (2006).
  - [10] A. O. Gogolin, and A. Komnik, Phys. Rev. Lett. **97**, 016602 (2006).
  - [11] A. Golub, Phys. Rev. B **73**, 233310 (2006).
  - [12] E. Sela and J. Malecki, Phys. Rev. B **80**, 233103 (2009).
  - [13] T. Fujii, J. Phys. Soc. Jpn. **79**, 044714 (2010).
  - [14] T. Delattre, C. Feuillet-Palma, L. G. Herrmann, P. Morfin, J.-M. Berroir, G. Fève, B. Plaçais, D. C. Glattli, M.-S. Choi, C. Mora, and T. Kontos, Nature Phys. **5**, 208 (2009).
  - [15] C. Mora, P. Vitushinsky, X. Leyronas, A. A. Clerk, and K. Le Hur, Phys. Rev. B **80**, 155322 (2009).
  - [16] R. Sakano, T. Fujii, and A. Oguri, Phys. Rev. B **83**, 075440 (2011).
  - [17] R. Sakano, A. Oguri, T. Kato and S. Tarucha, Phys. Rev. B **83**, 241301 (2011).
  - [18] R. Sakano, Y. Nishikawa, A. Oguri, A. C. Hewson, and S. Tarucha, Phys. Rev. Lett. **108**, 266401 (2012).
  - [19] H. R. Krishna-murthy, J. W. Wilkins, and K. G. Wilson, Phys. Rev. B **21**, 1003 (1980).
  - [20] W. Izumida, O. Sakai and Y. Shimizu, J. Phys. Soc. Jpn. **67**, 2444 (1998).
  - [21] P. Coleman, Phys. Rev. B **28**, 5255 (1983).
  - [22] N. Bickers, Rev. Mod. Phys. **59**, 845 (1987).
  - [23] A. Oguri, R. Sakano, and T. Fujii, Phys. Rev. B **84**, 113301 (2011).
  - [24] A. Oguri, Phys. Rev. B **85**, 155404 (2012).
  - [25] L. S. Levitov and M. Reznikov, Phys. Rev. B **70**, 115305 (2004).
  - [26] D. Bagrets, Y. Utsumi, D. Golubev, and G. Schön,

- Fortschr. Phys. **54**, 917 (2006).
- [27] M. Esposito, U. Harbola, and S. Mukamel, Rev. Mod. Phys. **81**, 1665 (2009).
- [28] K. Yamada, Prog. Theor. Phys. **53**, 970 (1975).
- [29] A. Yoshimori, Prog. Theor. Phys. **55**, 67 (1976).
- [30] V. Zlatić and B. Horvatić, Phys. Rev. B **28**, 6904 (1983).
- [31] Y. Nishikawa, D. J. G. Crow, and A. C. Hewson, Phys. Rev. B **82**, 115123 (2010).
- [32] A. C. Hewson, J. Phys.: Condens. Matter **13**, 10011 (2001).